Covalent organic/inorganic hybrid proton-conductive membrane with semi-interpenetrating polymer network: Preparation and characterizations

Rong-Qiang Fu [a], Jung-Je Woo [a], Seok-Jun Seo [a],
Jae-Suk Lee [b], Seung-Hyeon Moon [a],*

[a] *Department of Environmental Science and Engineering, Gwangju Institute of Science and Technology,
Gwangju 500-712, Republic of Korea*
[b] *Department of Materials Science and Engineering, Gwangju Institute of Science and Technology,
Gwangju 500-712, Republic of Korea*

Abstract

A series of new covalent organic/inorganic hybrid proton-conductive membranes, each with a semi-interpenetrating polymer network (semi-IPN), for direct methanol fuel cell (DMFC) applications is prepared through the following sequence: (i) copolymerization of impregnated styrene (St), *p*-vinylbenzyl chloride (VBC) and divinylbenzene (DVB) within a supporting polyvinyl chloride (PVC) film; (ii) reaction of the chloromethyl group with 3-(methylamine)propyl-trimethoxysilane (MAPTMS); (ii) a sol–gel process under acidic conditions; (iv) a sulfonation reaction. The developed membranes are characterized in terms of Fourier transform infrared/attenuated total reflectance (FTIR/ATR), scanning electron microscopy/energy-dispersive X-ray analysis (SEM/EDXA), elemental analysis (EA) and thermogravimetric analysis (TGA), which confirm the formation of the target membranes. The developed copolymer chains are interpenetrating with the PVC matrix to form the semi-IPN structure, and the inorganic silica is covalently bound to the copolymers. These features provide the membranes with high mechanical strength. The effect of silica content is investigated. As the silica content increases, proton conductivity and water content decrease, whereas oxidative stability is improved. In particular, methanol permeability and methanol uptake are reduced largely by the silica. The ratio of proton conductivity to methanol permeability for the hybrid membranes is higher than that of Nafion 117. All these properties make the hybrid membranes a potential candidate for DMFC applications.
© 2008 Elsevier B.V. All rights reserved.

Keywords: Proton-conductive membrane; Organic/inorganic hybrid membrane; Semi-interpenetrating polymer network; Direct methanol fuel cell
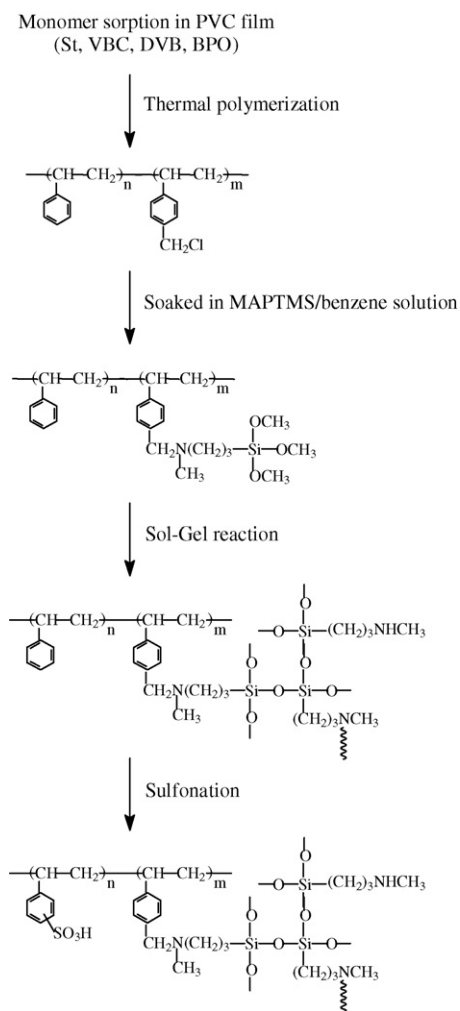
1. Introduction

Fuel cells have recently attracted considerable attention as an alternative energy-conversion technology [1]. Compared with conventional energy-conversion systems based on heat engines and fossil fuels, fuel cell systems directly transform chemical energy into electrical energy with the advantages of producing no waste products and causing no environmental problems. Among the various types of fuel cell, the direct methanol fuel cell (DMFC) is probably the most developed low-temperature system particularly for portable devices, such as laptops, handphones and personal digital assistants (PDAs). The DMFC has

no the problems of the difficult storage of hydrogen gas or a complex reforming auxiliary compared with the hydrogen-fuelled proton-exchange membrane fuel cell (PEMFC). One of the vital components of the DMFC is the proton-conductive membrane, which serves as a physical separator between the anode and the cathode with the function of transporting protons and blocking electrons. Nowadays, the most utilized proton-conductive membrane is Nafion, which is a perfluorinated polymeric membrane developed by DuPont in the late 1960s [2]. Although Nafion has high proton conductivity, excellent chemical stability and good mechanical strength for fuel cells operating below 90 °C, high methanol crossover and high cost restrict its large-scale industrial application. For this reason, a number of studies have been carried out to develop alternative membrane materials [3–6].

One interesting alternative is a hybrid organic/inorganic membrane which has the potential to provide unique combi-

Scheme 1. Chemical reactions in membrane preparation.

film, thereby forming a physical network. The two polymer chains become miscible due to the semi-IPN structure, and a high mechanical stability can be achieved from the supporting film whereas the propagated polymer chains bring the proton conductivity after a post-sulfonation reaction.

In this research, the above two concepts, covalent organic/inorganic hybrid and semi-IPN technology, are combined together to develop a series of new proton-conductive membranes. Fig. 1 schematically illustrates the preparation procedures and Scheme 1 shows the corresponding chemical reactions. The non-porous supporting polyvinyl chloride (PVC) film is swollen in the monomer solution containing styrene (St), p-vinylbenzyl chloride (VBC) and divinylbenzene (DVB). The impregnated monomers are thermally polymerized within the PVC film, thereby forming a semi-IPN structure. The chloromethyl groups in VBC then react with 3-(methylamine)propyl-trimethoxysilane (MAPTMS). After a sol–gel process, the developed inorganic $\equiv$Si–O– network is covalently bound to the organic poly(St-co-VBC) network. A covalent organic/inorganic hybrid proton-conductive membrane with a semi-IPN structure is obtained after a subsequent sulfonation reaction. Styrene has been chosen due to its high thermal stability and suitability for the sulfonation process of the aromatic ring to incorporate the sulfonic group responsible for high proton conductivity [8,11]. The developed membranes are then characterized in terms of Fourier transform infrared/attenuated total reflectance (FTIR/ATR), scanning electron microscopy/energy-dispersive X-ray analysis (SEM/EDXA), elemental analysis (EA), thermogravimetric analysis (TGA), ion-exchange capacity, water content, methanol uptake, proton conductivity, methanol diffusivity, mechanical stability and oxidative stability.

2. Experimental

2.1. Materials

A PVC film was supplied by Hwashin Engineering Co. (Seoul, Korea) with a thickness of 80 μm. Styrene, VBC and DVB were supplied by Aldrich (Milwaukee, WI, USA) and then purified with Aldrich inhibitor removers. The thermal initiator benzoyl peroxide (BPO) from Fluka (Buchs, Switzerland) was purified by recrystallization in a methanol/water mixture at −5 °C. MAPTMS and chlorosulfonic acid from Aldrich, 1,2-dichloroethane from Junsei Chemical Co. (Tokyo, Japan) and other reagents were used as received.

2.2. Membrane preparation

As shown in Scheme 1, the membrane preparation procedures can be divided into four steps. The first step is thermal polymerization. The PVC film was cleaned in n-hexane for 4 h before it was soaked in a monomer solution of St, VBC, DVB and BPO for 3 h at room temperature. The monomer-swollen PVC film was placed between two glass plates and sealed with aluminum foil to prevent the evaporation of the monomers. Thermal polymerization was carried out in an oven at 80 °C for 8 h. During

nations of organic and inorganic properties [7,8]. The organic component may provide mechanical strength and proton conductivity, whereas the inorganic phase can reduce methanol permeation and improve both thermal and chemical stability. Furthermore, in order to control the dosage and dispersion of the inorganic component and make it more compatible with the organic phase, a covalent linking could be designed and formed between the two phases. For example, a covalent organic/inorganic hybrid material was synthesized with 2-hydroethyl methacrylate (HEMA) as a covalent-bonding agent: the hydroxyl group in HEMA polycondensed with prehydrolyzed tetraethyl orthosilicate (TEOS), while the C=C double bond copolymerized with styrene [8,9]. The monolithic membrane from the sulfonated hybrid material was, however, too brittle and too mechanically weak when the inorganic content was relatively high.

The mechanical strength of the membrane could be enhanced by utilizing a semi-interpenetrating polymer network (semi-IPN) technology based on a supporting film and a monomer solution [10]. In this method, the impregnated monomer within the supporting film is polymerized, and the propagated polymer chains are interpenetrated with those of the supporting
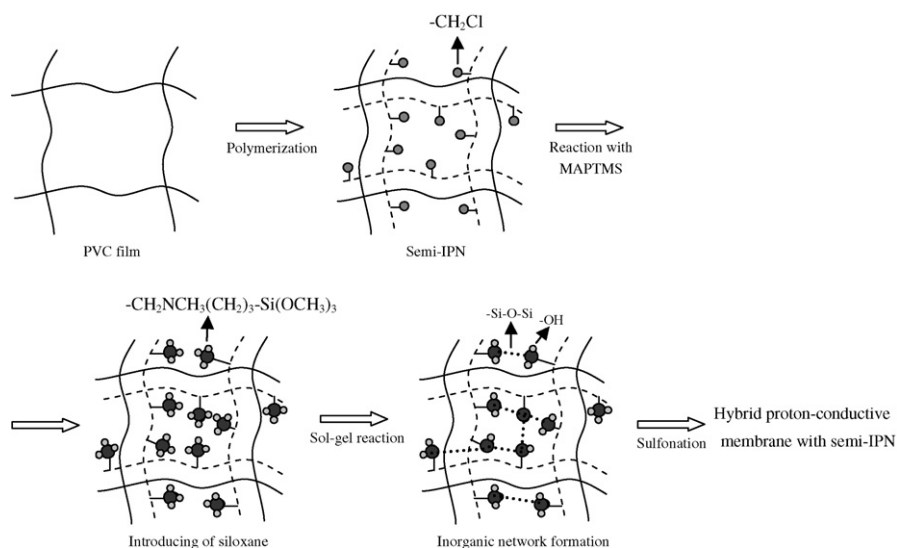
Fig. 1. Proposed preparation procedures.

the second step, the film was soaked in a MAPTMS/benzene solution for 24 h. MAPTMS diffused into the benzene-swollen film and its amine group reacted with the chloromethyl group of VBC. The film was then washed in benzene for 1 h to remove excess MAPTMS. The third step was a sol–gel reaction under acidic conditions. The film was soaked in 0.05N HCl for 3 h; meanwhile, the methoxyl groups were partially hydrolyzed. The full hydrolyzation–polycondensation reaction was carried out by placing the film in an oven at 80 °C for 12 h and then at 100 °C for 1 h. Finally, the pre-swollen film in 1,2-dichloroethane was sulfonated in a mixed solution of chlorosulfonic acid and 1,2-dichloroethane (10:90, v/v) at room temperature for 1 h, and then washed with acetone and purified water. The film was subsequently soaked in 1.0N NaOH solution for 12 h, re-acidified in 1.0N HCl for 12 h, and washed completely in purified water for ready use.

As listed in Table 1, four semi-IPN hybrid membranes were prepared with 5–30% VBC content in monomer solution and 10% MAPTMS in benzene. As a reference, a semi-IPN silica-free membrane (M-0) was also produced.

2.3. Characterization

2.3.1. FTIR/ATR, SEM/EDXA, EA and TGA

Fourier transform infrared/attenuated total reflectance spectra of the membrane were obtained with a Jasco 460 plus spectrometer (Tokyo, Japan). The membrane's fractured surface was observed by means of field emission scanning electron microscopy (FE-SEM, Jeol Model JSF 6340F, Tokyo, Japan), and the distribution of C, N, Si and S atoms in the thickness direction was determined by energy-dispersive X-ray analysis. The elemental analysis was carried out using an elemental analyzer (FlashEA 1112 series, Thermo Electron Corporation) at a combustion temperature of 1100 °C, and the thermogravimetric analysis was undertaken with a TA Instruments TGA 2050 system using a heating rate of 10 °C min^{-1} in air atmosphere over a temperature range of 50–800 °C.

2.3.2. Ion-exchange capacity

Ion-exchange capacity (IEC) was determined by the back-titration method. The membrane in proton form was soaked in 0.01 mol l^{-1} NaOH solution for 24 h. The reduction in alkalinity of the NaOH solution was determined by titration with 0.01 M HCl solution. The IEC was calculated as the ratio of the reduction in alkalinity to the weight of dry membrane.

2.3.3. Water content and methanol uptake

To measure the water-swelling property, the membrane was soaked in distilled water for 24 h, taken out and wiped with a filter paper, and then weighed immediately. The sample was then dried under vacuum conditions at 50 °C until a constant weight was obtained. The water content was determined as the ratio of the absorbed water to membrane dry weight. The methanol uptake was determined using the same method, except that the sample was soaked in pure methanol and the methanol uptake was calculated as the ratio of the absorbed methanol to membrane dry weight.

2.3.4. Proton conductivity

The proton conductivity was measured using the normal four-probe technique [12,13]. The Teflon measuring cell consisted of two stainless-steel current-carrying electrodes (2 cm apart) and two platinum wire potential-sensing electrodes (1 cm apart). A 1-cm wide and 4-cm long membrane strip was mounted into the cell. The impedance was determined using an Autolab PGSTAT 30 (Eco Chemie, the Netherlands) over a frequency range from 1 MHz to 50 Hz. Using a Bode plot, the frequency region over which the impedance had a constant value was checked, and the resistance was then obtained from a Nyquist plot. Proton conductivity (κ) was calculated according to the following expression:

$$\kappa = \frac{L}{RWd} \tag{1}$$

where R is the membrane resistance, L the distance between potential-sensing electrodes, W and d are the width and thickness

Table 1
Composition of membranes

Membrane	Monomer composition, St/VBC/DVB (v/v, %)	MAPTMS concentration in benzene (v/v, %)	BPO addition
M-0	95/0/5	0	3.0 g per 100 ml monomeric solution
M-5	90/5/5	10	3.0 g per 100 ml monomeric solution
M-10	85/10/5	10	3.0 g per 100 ml monomeric solution
M-20	75/20/5	10	3.0 g per 100 ml monomeric solution
M-30	65/30/5	10	3.0 g per 100 ml monomeric solution

of the membrane, respectively. During measurement, the cell was soaked in purified water, and so proton conductivity was for the fully hydrated membrane at room temperature.

2.3.5. Methanol permeability

Methanol permeability measurement was carried out with a home-made permeation measuring cell that had two compartments. Compartment A was filled with 150 ml 20% (v/v) methanol solution in de-ionized water, and compartment B was filled with 150 ml de-ionized water. The membrane was mounted between the two compartments, and the diameter of the diffusion area was 1.0 cm. The solutions in both compartments were magnetically stirred. The methanol concentration in compartment B was monitored using a refractive index detector (RI750F, Younglin Instrument Co., Korea) through a 1-mm-diameter silicon tube with a 1.0 ml min^{-1} constant flow driven by a Masterflex pump. The output signal was converted by a data module (Autochro, Younglin Instrument Co., Korea) and recorded by a personal computer.

Methanol permeability (P) was obtained by means of the following relationship [13]:

$$C_B(t) = \frac{A}{V_B} \frac{P}{L} C_A(t - t_0) \qquad (2)$$

where C_A is the initial methanol concentration in compartment A; $C_B(t)$ the methanol concentration in compartment B at diffusion time t; V_B the volume of de-ionized water in compartment B; L the thickness of the membrane; A is the effective permeating area.

2.3.6. Mechanical testing

The tensile strength and elongation at break of the wet membrane was measured using the Instron model 5567 universal testing machine according to the ASTM method D-882-79. In the measurement, 2 cm × 5 cm dumbbells were tested in a flat-faced grip initially spaced 2 cm apart with a crosshead speed of 2.54 cm min^{-1}.

2.3.7. Oxidative stability

The oxidative stability was characterized by measuring the weight change of the membrane when soaked in an aqueous H$_2$O$_2$ solution [14]. The membrane strip with a size of 1 cm × 4 cm was immersed in 3 wt.% H$_2$O$_2$ aqueous solution at 60 °C. During immersion, the membranes were intermittently taken out of the solution at 12 h periods and weighed after wiping off the surface water. The variation of membrane weight vs. time was plotted to evaluate the oxidative stability.

3. Results and discussion

3.1. Membrane preparation

The chemical reactions during the preparation of hybrid membrane M-10 were investigated by FTIR/ATR spectra, as presented in Fig. 2. After polymerization, new absorption peaks were observed at 1600 and 1491 cm^{-1} and assigned to the aromatic groups, which indicates that monomers are polymerized within the PVC film and so a semi-IPN is well formed. After the sol–gel process, there is a broad absorption band centred at 1100 cm^{-1} and is attributed to a Si–O–Si stretching vibration, which shows the successful import of the inorganic component. In the sulfonated sample, absorption bands assigned to sulfonic acid groups are observed at 1123 and 1004 cm^{-1}, and peaks for S=O stretching vibration are observed at 1369 and 1169 cm^{-1}. The FTIR/ATR results demonstrate that a hybrid proton-conductive membrane with semi-IPN is successfully prepared. Although there is no direct information from the spectra on the covalent linking between organic and inorganic components due to the difficult recognition of the C–N vibration in –C$_6$H$_4$CH$_2$–NCH$_3$(CH$_2$)$_3$–Si≡, some conclusions are possible as follows. First, the reactions between polymers containing chloromethyl groups and different kinds of amines with high steric hindrance have been successfully conducted [15–17]. The same reaction between –CH$_2$Cl and =NH may occur in this study. Second, it should be noted that the film is swollen in benzene during the second step of membrane preparation and MAPTMS can easily diffuse into the film. The adsorbed
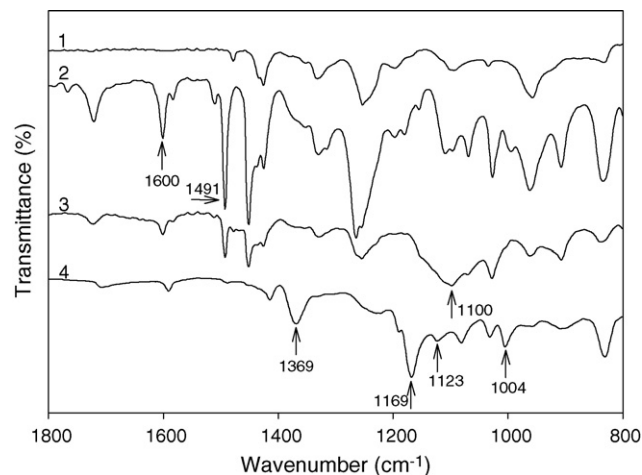

Fig. 2. FTIR/ATR spectra of hybrid membrane M-10: (1) PVC film; (2) after polymerization; (3) after sol–gel process; (4) after sulfonation.

MAPTMS is then removed by washing the film in benzene. As shown in FTIR spectra and in EA and TGA (to be presented later in this study), however, the final membrane has sufficient silica content. The third conclusion is that membranes prepared from monomer solutions with different VBC content have different silica content, which will be further discussed in this study.

The fractured surface of the hybrid membrane M-30 was also investigated by EDXA. It is found that the distributions of the C, N, Si and S are nearly uniform in the thickness direction, i.e., the contents in the middle are not lower than those near the surface. The uniform distributions of the N and Si elements indicate the successful import of MAPTMS during the second step of membrane preparation because these two elements come from only MAPTMS. The uniform distribution of S confirms a successful sulfonation reaction.

It is necessary to examine the silica content in the final membranes. As both silicon and nitrogen elements derive from MAPTMS, the molar contents of these two elements are the same according to the formula of MAPTMS. The nitrogen content was obtained in EA, and so the silica content could be calculated, as listed in Table 2. With increase in VBC content, the silica content also increases. Consequently, the ratio of the reacted chloromethyl group could be estimated. In this estimation, the following assumptions are made. (i) The produced polymer chains have the same composition as that of the monomer solution. This assumption is based on the fact that all adsorbed monomers are polymerized completely. (ii) When the film is immersed in the MAPTMS/benzene solution, MAPTMS prefers to react with VBC rather cause hydrolyzation–polycondensation. The waterless condition without any catalyst (acid or base) makes the assumption reasonable. (iii) All –Si(OCH$_3$) groups are converted to silica during the sol–gel process. (iv) No side reactions are observed during the sulfonation reaction. Furthermore, for all the prepared membranes, the weight-gain ratio during the thermal polymerization has been measured as about 60%. Based on the above assumptions and facts, the MAPTMS content can be estimated from the silica content and ion-exchange capacity (shown in Fig. 4), as shown in Table 2. The ratio of MAPTMS to VBC in M-5 was 1.25, which means that in the case of low VBC content: (i) all chloromethyl groups are reacted and (ii) partial hydrolyzation–polycondensation takes place when the film is immersed in the MAPTMS/benzene solution or the adsorbed MAPTMS is not removed completely by washing the film in benzene. By contrast, the ratio is lower than unity for M-20 and M-30, which indicates that there are unreacted –CH$_2$Cl at a high VBC content, which probably results from a hindrance to the diffusion of MAPTMS into the benzene-swollen semi-IPN. It is also found that the final membranes have different silica content, and the silica content increases with increase in VBC content, as shown by the ratio of MAPTMS to PVC film. Thus it can be inferred that MAPTMS molecules diffusing into membranes react readily with VBC, and then covalent linkages between organic and inorganic components are formed during the sol–gel process.

The thermal properties of the prepared membranes were examined through TGA, and the results are given in Fig. 3. The
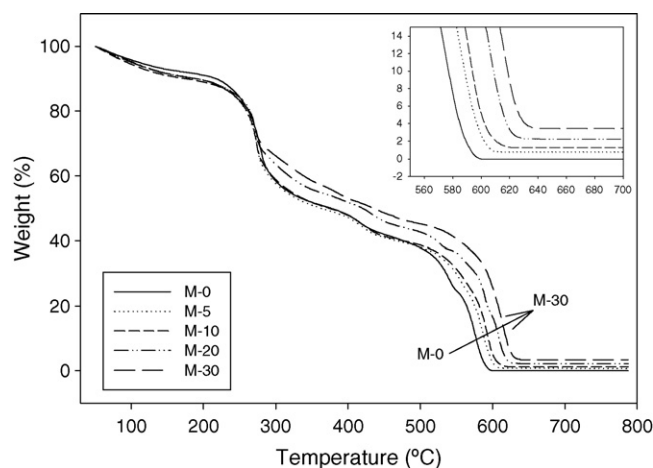

Fig. 3. TGA curves of prepared membranes.

weight loss below 240 °C is attributed to desorption of moisture and residual solvents. The next weight loss corresponds to thermal desulfonation, thermal degradation and thermal oxidation of PVC and the copolymer chains. Though the hybrid membranes show no obvious enhancement in thermal stability, possibly because of the degradation of the supporting PVC material [18], all the membranes can be used at temperatures lower than 240 °C. A further notable feature of the TGA results is the residual content at 750 °C (listed in Table 2). It is reasonable to assume that the only residue is silica at this temperature [15], and so the ratio of the reacted chloromethyl group can be estimated. In general, the values estimated from TGA are consistent with those from EA. As expected, the silica content increases with increasing VBC content.

3.2. Ion-exchange capacity

Ion-exchange capacity provides an indication of the content of sulfonic acid groups in the membrane. The IEC values of the prepared membranes are presented in Fig. 4. As a reference, the value for a Nafion 117 membrane has also been determined. Although the hybrid membranes consist of support material, the IEC values range from 1.71 to 2.45 meq g^{-1} and are much
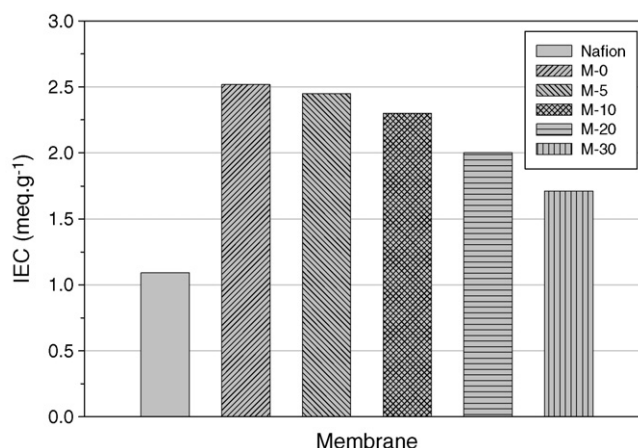

Fig. 4. Ion-exchange capacity of prepared membranes.

Table 2
Estimated MAPTMS contents from nitrogen content in EA and residues in TGA

Membrane	St/VBC/DVB (by mol)	Elemental analysis (EA)				Thermogravimetric analysis (TGA)		
		N (wt.%)	SiO$_2$ (wt.%)	Ratio of MAPTMS to VBC	Ratio of MAPTMS to PVC	SiO$_2$ (wt.%) (residue at 750 °C)	Ratio of MAPTMS to VBC	Ratio of MAPTMS to PVC
M-5	22.4/1.0/1.0	0.20	0.86	1.25	0.29	0.78	1.13	0.26
M-10	21.1/2.0/1.0	0.34	1.46	1.06	0.49	1.27	0.92	0.42
M-20	18.6/4.0/1.0	0.58	2.49	0.91	0.82	2.26	0.83	0.75
M-30	16.2/6.1/1.0	0.88	3.77	0.94	1.24	3.46	0.85	1.14

higher than that of Nafion. This shows that the hybrid membranes contain sufficient sulfonic acid sites for the intended proton transportation. The IEC value decreases as the VBC content (or silica content) increases, which is attributed to a reduction in the number of suitable sulfonating sites (note, bi-subsituted VBC is difficult to be sulfonated due to steric hindrance) and also to a decrease in the degree of swelling [19]. The silica component makes the membrane rigid, and the swelling of the polymer network is suppressed. Therefore, it becomes more difficult for chlorosulfonic acid to react with the inner polymer network chains, which leads to less sulfonic acid groups being attached to the aromatic rings.

3.3. Water content and methanol uptake

The water contents of the hybrid membranes and the Nafion membrane are shown in Fig. 5. The prepared membranes have higher water content than Nafion, presumably due to the higher amount of sulfonic acid groups with their strong affinity to water. The water content in the silica-free membrane (M-0) is highest, and those of the other membranes decrease as the silica content is increased. The effect of silica on water content introduces two contradicting aspects: (i) a hygroscopic effect [20] due to the unreacted –Si–OH group and the increasing site for bound water, which would increase the content of bound water; (ii) a crosslinking effect due to the inorganic network [21], which would reduce polymer chain mobility (free volume) and the space where absorbed water could be accommodated.
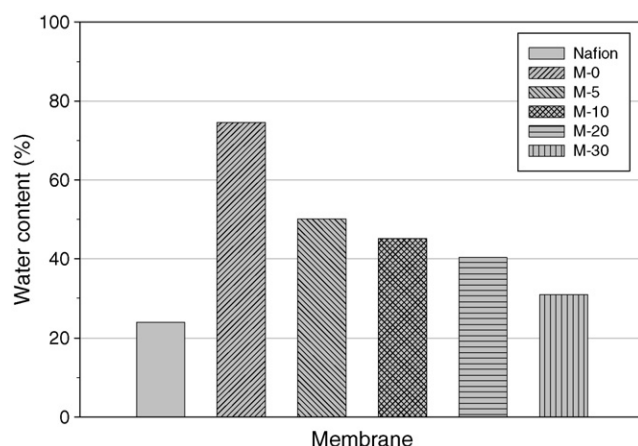
In this study, the crosslinking effect is more prominent than the hygroscopic effect, and so the total water content decreases with increasing silica content.

Methanol uptake of the membranes is presented in Fig. 6. Compared with a Nafion membrane, which has as high as 82% methanol uptake, the prepared membranes have much lower methanol uptake. This is totally different from the behaviour of water uptake. The methanol uptake decreases as the silica content is increased. The cause can be explained in terms of the membrane structure. The main chains of the Nafion membrane are well organized with flexible linear fluorinated chains that have long-grafted ionic groups. By contrast, the prepared membranes have the semi-IPN structure with an inorganic silica network and this results in a lower swelling ability than that of Nafion. The low methanol uptake indicates that the hybrid membranes are dimensionally stable when used in a DMFC.

3.4. Proton conductivity

The proton conductivity of the fuel cell membrane is a key property that directly affects operational fuel cell voltage [1]. Fig. 7 shows the proton conductivities of the hybrid membranes and the Nafion membrane. The proton conductivity of the silica-free membrane (M-0) is 0.10 S cm^{-1}, i.e., slightly higher than that of the Nafion samples (0.08 S cm^{-1}). As the silica content is increased, the proton conductivity of hybrid membranes decrease. It is believed that proton conduction in the membranes proceeds mainly by the Grotthus mechanism, i.e., protons

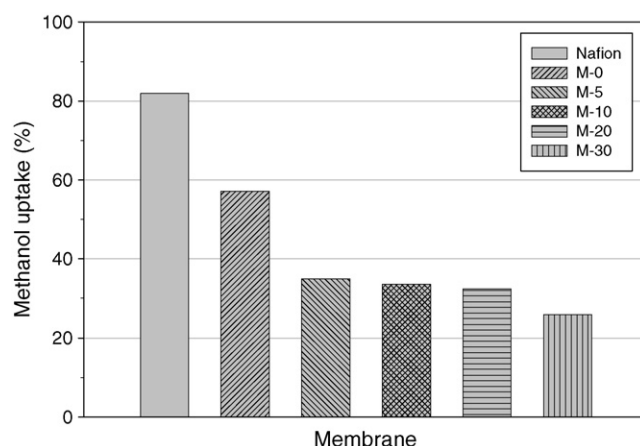Fig. 5. Water content of prepared membranes.

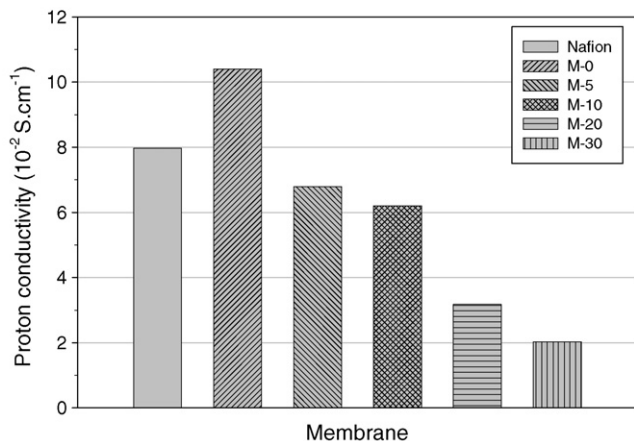Fig. 6. Methanol uptake of prepared membranes.

Fig. 7. Proton conductivity of prepared membranes.

transport down a chain of water molecules [22]. This mechanism predicts that proton-conductivity depends much on both the water and sulfonic group content. As described above, both decrease with silica content, hence it is a reasonable result that proton conductivity also decreases.

Proton conductivity may be affected by the testing medium. Thus the membranes were also immersed in 10 vol.% methanol solution (the concentration that is generally used in a DMFC) to measure the proton conductivities. It is found that the hybrid membranes and the Nafion membrane have similar but no preferential behaviours: all the proton-conductivities decrease about 8% compared the data for pure water. The decreasing of proton conductivity is due to the intrinsic molecular differences of methanol and water (e.g., the dipole momentum of methanol and water is, respectively, 1.70 and 1.85 Debye [23]) and the different interactions with protons.

3.5. Methanol permeability

To evaluate the practicality of hybrid membranes for DMFCs, methanol permeability was measured and is shown in Fig. 8. The permeability of Nafion and the silica-free membrane (M-0) is 1.86×10^{-6} and 1.23×10^{-6} cm^2 s^{-1}, respectively. With
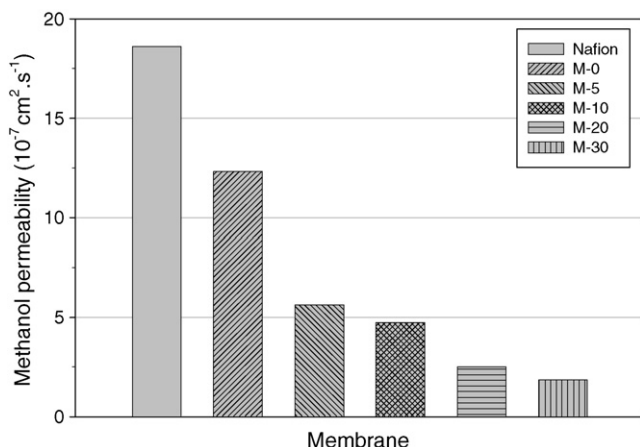

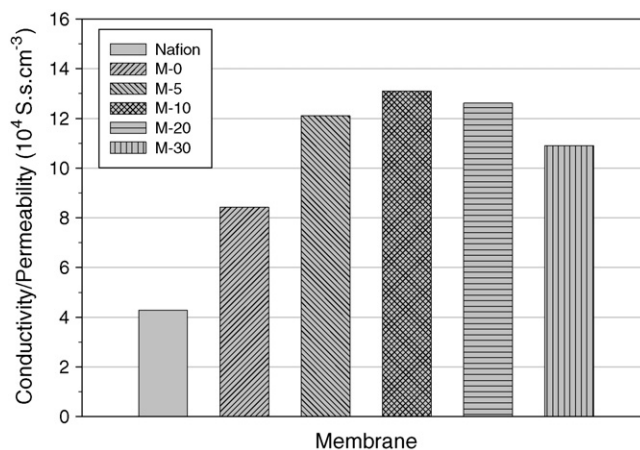Fig. 8. Methanol permeability of prepared membranes.

Fig. 9. Ratio of proton conductivity to methanol permeability of prepared membranes.

increase of silica in the hybrid membranes, the methanol permeability decreases sharply. For M-30, the permeability is only 1.85×10^{-7} cm^2 s^{-1}, i.e., 10 times lower than that of Nafion. This shows that the inorganic component can be used as a means to obstruct methanol transportation. This behaviour can be explained as follows. With increase in silica content, the polymer chain mobility and swelling of the networks in aqueous methanol solution decrease, which reduces the channels to pass methanol molecules so that resistance to the diffusion of methanol is increased.

For DMFC application, the optimum proton-conductive membrane should have the lowest methanol permeability and the highest proton conductivity. Nevertheless, many studies on polymer membranes have revealed a tendency for the decrease in methanol permeability to be accompanied by a decrease in proton conductivity [19,21,24]. Thus, a compromise between these properties has to be achieved. A characteristic factor, Φ, used to evaluate membrane performance in a DMFC application can be calculated using the following expression:

$$\Phi = \frac{\kappa}{P} \tag{3}$$

where κ is the proton conductivity and P is the methanol permeability. From the proton conductivity data and methanol permeability data shown in Figs. 7 and 8, the characteristic factors were calculated, as shown in Fig. 9. All the prepared membranes have a higher Φ value than that of Nafion. This is attributed to the inorganic component and the semi-IPN structure. The highest Φ is found with M-10, although its proton conductivity and methanol permeability are mild. The highest value indicates that the desired compromise has been achieved: the silica component reduces the methanol permeability without a large sacrifice of proton conductivity.

3.6. Mechanical properties

The mechanical stability was measured in terms of tensile strength and elongation at break, as presented in Fig. 10. The prepared membranes have a relatively high tensile strength, which results from the semi-IPN structure (the tensile strength of the
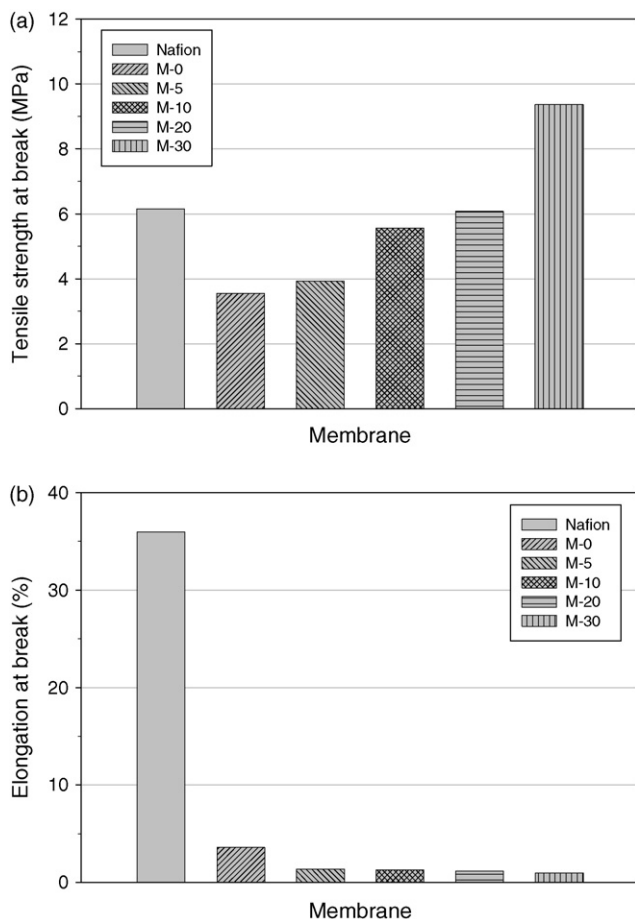
Fig. 10. (a) Tensile strength and (b) elongation at break of prepared membranes.

Fig. 11. Oxidative stability of prepared membranes.

PVC film with $100\,\mu m$ thickness is about $50\,MPa$ [10]). The tensile strength is enhanced by the silica component, e.g., M-30 has a higher strength than Nafion. The mechanical strength should be sufficient for fuel cell applications. Due to plasticization of the linear structure, however, Nafion had a much higher elongation at break than the prepared membranes.

3.7. Oxidative stability

Finally, the oxidative stability of the hybrid membranes was evaluated. During fuel cell operation, possible degradation of the polymer electrolyte is caused by oxygen diffusing through the membrane and undergoing incomplete reduction at the anode to form $HO^\bullet$ and $HO_2^\bullet$ radicals [25]. For polystyrene membranes, these radicals attack the tertiary hydrogen at the α-carbon to cause considerable degradation. Testing the lifetime of polymer electrolyte membranes in actual fuel cells is both time-consuming and expensive. Thus, it is desirable to develop and utilize rapid and simple methods. Guo et al. [26] chose aqueous $3\,wt.\%$ H_2O_2 solution containing $4\,ppm$ Fe^{2+} at $68\,^\circ C$ to evaluate the oxidative stability of membranes. For those based on polystyrene, it was found that decomposition occurred within several hours [14]. Therefore, a more moderate testing should be used. In this study, the oxidative stability was assessed in a $3\,wt.\%$ H_2O_2 aqueous solution without any Fe^{2+} at $60\,^\circ C$.
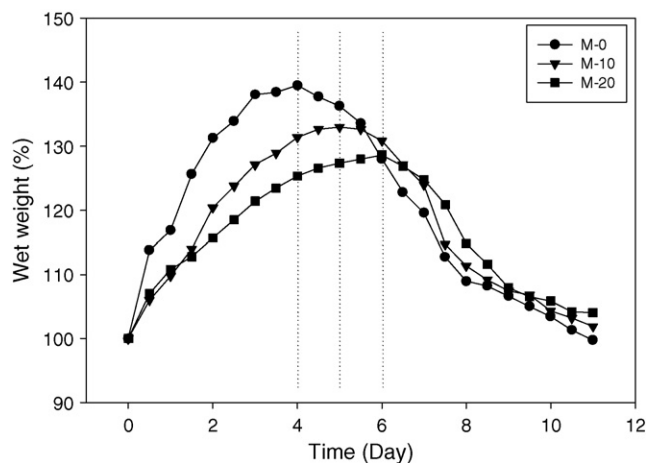
As a working hypothesis, the PVC backbone is assumed to be more stable than sulfonated poly(St-co-VBC). As shown in Fig. 11, the membrane weight first increased and then decreased, which is similar to the results obtained by Chen et al. [14]. There are two contrary effects when soaking a membrane in oxidative solution. One is degradation of sulfonated poly(St-co-VBC) chains, which decreases the membrane weight. The other is swelling due to degradation of the DVB and silica crosslinking structure, which increases the membrane weight. With the latter effect, permeation of H_2O_2 into the membrane becomes easier and so the decomposition of polystyrene chains becomes faster. When the decomposition rate increases continuously and is larger than the swelling effect, the wet weight of the membrane exhibits a peak value. With increase in silica content, the wet weight at the peak is decreased. For the membrane with high silica, the crosslinking structure is only partially degraded at the peak value of membrane weight. Thus, the swelling effect of higher-silica membrane is lower. Here, the oxidative stability is characterized by the durability time, which is defined as the period that elapses before the weight reaches its peak value. The silica increases the oxidative stability due to its crosslinking effect. As reflected by the water content, the silica renders the membrane more compact. This restricts the diffusive ingress of $HO^\bullet$ radicals and reduces their attack on the polymer chain. The effect is similar to the crosslinking by DVB, which greatly improves the stability of polystyrene-grafted polymer electrolytes [27,28].

4. Conclusions

New covalent organic/inorganic hybrid proton-conductive membranes with a semi-IPN structure have been obtained through the polymerization of monomers within a supporting PVC film, followed by the introduction of siloxane, a sol–gel process and a sulfonation reaction. Characterization studies with FTIR/ATR, SEM/EDXA, EA and TGA confirm the formation of the target membranes. The membranes possess good electrochemical properties for fuel cell applications, as well as reasonable mechanical strength and oxidative stability.

As the content of silica is increased, both proton conductivity and water content decrease whereas oxidative stability is improved. Methanol permeability and methanol uptake are markedly reduced in the presence of silica; the associated characteristic factor Φ of the hybrid membrane is higher than that of Nafion 117. All these properties make the hybrid membrane a potential candidate for DMFC applications.

Acknowledgment

References

[1] J. Larminie, A. Dicks, Fuel Cell Systems Explained, 2nd ed., John Wiley & Sons Ltd., 2003.
[2] K.A. Mauritz, R.B. Moore, Chem. Rev. 104 (2004) 4535–4585.
[3] J.A. Kerres, J. Membr. Sci. 185 (2001) 3–27.
[4] M.A. Hickner, H. Ghassemi, Y.S. Kim, B.R. Einsla, J.E. McGrath, Chem. Rev. 104 (2004) 4587–4612.
[5] N.W. Deluca, Y.A. Elabd, J. Polym. Sci., Part B: Polym. Phys. 44 (2006) 2201–2225.
[6] V. Neburchilov, J. Martin, H. Wang, J. Zhang, J. Power Sources 169 (2007) 221–238.
[7] J. Wen, G.L. Wilkes, Chem. Mater. 8 (1996) 1667–1681.
[8] M. Aparicio, A. Duran, J. Sol–Gel Sci. Technol. 31 (2004) 103–107.
[9] M. Aparicio, Y. Castro, A. Duran, Solid State Ionics 176 (2005) 333–340.
[10] Y.J. Choi, M.S. Kang, S.H. Moon, J. Appl. Polym. Sci. 88 (2003) 1488–1496.
[11] S.G. Ehrenberg, J.M. Serpico, G.E. Wnek, J.N. Rider, Fuel cell incorporating novel ion-conducting membrane, U.S. Pat. 5,679,482 (1997).
[12] Y. Sone, P. Ekdunge, D. Simonsson, J. Electrochem. Soc. 143 (1996) 1254–1259.
[13] Y. Woo, S.Y. Oh, Y.S. Kang, B. Jung, J. Membr. Sci. 220 (2003) 31–45.
[14] J.H. Chen, M. Asano, T. Yamaki, M. Yoshida, J. Membr. Sci. 269 (2006) 194–204.
[15] S.L. Zhang, C.M. Wu, T.W. Xu, M. Gong, X.L. Xu, J. Solid State Chem. 178 (2005) 2292–2300.
[16] E.N. Komkova, D.F. Stamatialis, H. Strathmann, M. Wessling, J. Membr. Sci. 244 (2004) 25–34.
[17] T. Sata, K. Teshima, T. Yamaguchi, J. Polym. Sci., Part A: Polym. Chem. 34 (1996) 1475–1482.
[18] J. Liggat, in: J. Brandrup, E.H. Immergut, E.A. Grulke (Eds.), Polymer Handbook, John Willey & Sons Inc., New York, 1999.
[19] J.-P. Shin, B.-J. Chang, J.-H. Kim, S.-B. Lee, D.-H. Suh, J. Membr. Sci. 251 (2005) 247–254.
[20] N. Miyake, J.S. Wainright, R.F. Savinell, J. Electrochem. Soc. 148 (2001) A898–A904.
[21] D.S. Kim, H.B. Park, J.W. Rhim, Y.M. Lee, Solid State Ionics 176 (2005) 117–126.
[22] B.S. Pivovar, Y.X. Wang, E.L. Cussler, J. Membr. Sci. 154 (1999) 155–162.
[23] D.R. Lide, Handbook of Chemistry and Physics, 87th ed., CRC Press, 2006–2007.
[24] J.-W. Rhim, H.-B. Park, C.-S. Lee, J.-H. Jun, D.-S. Kim, Y.-M. Lee, J. Membr. Sci. 238 (2004) 143–151.
[25] G. Hünner, E. Roduner, J. Mater. Sci. 9 (1999) 409–418.
[26] Q.-H. Guo, P.N. Pintauro, H. Tang, S. O'Connor, J. Membr. Sci. 154 (1999) 175–181.
[27] J.-H. Chen, M. Asano, T. Yamaki, M. Yoshida, J. Mater. Sci. 41 (2006) 1289–1292.
[28] L. Gubler, S.A. Gursel, G.G. Scherer, Fuel Cells 5 (2005) 317–335.